Research Article | Vol. 24, No. 18 | 5 Sep 2016 | OPTICS EXPRESS 20696

Optics EXPRESS

Localized surface plasmon for enhanced lasing performance in solution-processed perovskites

TSUNG SHENG KAO,[1] KUO-BIN HONG,[1] YU-HSUN CHOU,[2] JIONG-FU HUANG,[1] FANG-CHUNG CHEN,[1,3] AND TIEN-CHANG LU[1,*]

[1]*Department of Photonics and Institute of Electro-Optical Engineering, National Chiao Tung University, Hsinchu 30010, Taiwan*
[2]*Institute of Lighting and Energy Photonics, College of Photonics, National Chiao Tung University, Tainan 71150, Taiwan*
[3]*fcchen@mail.nctu.edu.tw*
[*]*timtclu@mail.nctu.edu.tw*

Abstract: A promising method to promote the lasing performance of solution-processed organic-inorganic lead-halide perovskites has been demonstrated. With the adding Ag and PMMA thin films, the threshold excitation power for low-temperature lasing action in perovskites can be greatly reduced by over two orders of magnitude than that acquired in bare perovskite layers, ascribing to the strong exciton-plasmon coupling between the Ag and perovskite films. Also, the PMMA layer can be exploited to prevent the perovskite degradation from the hydrolysis in ambient environment, achieving long-lasting light-emitting performance. The advantages exhibited by the hybrid perovskite configuration would be very promising in making practical laser devices.

OCIS codes: (250.5403) Plasmonics; (300.6360) Spectroscopy, laser; (160.3380) Laser materials.

References and links

1. A. Kojima, K. Teshima, Y. Shirai, and T. Miyasaka, "Organometal halide perovskites as visible-light sensitizers for photovoltaic cells," J. Am. Chem. Soc. **131**(17), 6050–6051 (2009).
2. J.-H. Im, C.-R. Lee, J.-W. Lee, S.-W. Park, and N.-G. Park, "6.5% efficient perovskite quantum-dot-sensitized solar cell," Nanoscale **3**(10), 4088–4093 (2011).
3. M. M. Lee, J. Teuscher, T. Miyasaka, T. N. Murakami, and H. J. Snaith, "Efficient hybrid solar cells based on meso-superstructured organometal halide perovskites," Science **338**(6107), 643–647 (2012).
4. M. Liu, M. B. Johnston, and H. J. Snaith, "Efficient planar heterojunction perovskite solar cells by vapour deposition," Nature **501**(7467), 395–398 (2013).
5. F. Hao, C. C. Stoumpos, D. H. Cao, R. P. H. Chang, and M. G. Kanatzidis, "Lead-free solid-state organic-inorganic halide perovskite solar cells," Nat. Photonics **8**(6), 489–494 (2014).
6. S. D. Stranks and H. J. Snaith, "Metal-halide perovskites for photovoltaic and light-emitting devices," Nat. Nanotechnol. **10**(5), 391–402 (2015).
7. H. Zhou, Q. Chen, G. Li, S. Luo, T.-B. Song, H.-S. Duan, Z. Hong, J. You, Y. Liu, and Y. Yang, "Interface engineering of highly efficient perovskite solar cells," Science **345**(6196), 542–546 (2014).
8. W. S. Yang, J. H. Noh, N. J. Jeon, Y. C. Kim, S. Ryu, J. Seo, and S. I. Seok, "High-performance photovoltaic perovskite layers fabricated through intramolecular exchange," Science **348**(6240), 1234–1237 (2015).
9. G. Xing, N. Mathews, S. S. Lim, N. Yantara, X. Liu, D. Sabba, M. Grätzel, S. Mhaisalkar, and T. C. Sum, "Low-temperature solution-processed wavelength-tunable perovskites for lasing," Nat. Mater. **13**(5), 476–480 (2014).
10. F. Deschler, M. Price, S. Pathak, L. E. Klintberg, D.-D. Jarausch, R. Higler, S. Hüttner, T. Leijtens, S. D. Stranks, H. J. Snaith, M. Atatüre, R. T. Phillips, and R. H. Friend, "High photoluminescence efficiency and optically pumped lasing in solution-processed mixed halide perovskite semiconductors," J. Phys. Chem. Lett. **5**(8), 1421–1426 (2014).
11. T. S. Kao, Y.-H. Chou, C.-H. Chou, F.-C. Chen, and T.-C. Lu, "Lasing behaviors upon phase transition in solution-processed perovskite thin films," Appl. Phys. Lett. **105**(23), 231108 (2014).
12. H. Zhu, Y. Fu, F. Meng, X. Wu, Z. Gong, Q. Ding, M. V. Gustafsson, M. T. Trinh, S. Jin, and X.-Y. Zhu, "Lead halide perovskite nanowire lasers with low lasing thresholds and high quality factors," Nat. Mater. **14**(6), 636–642 (2015).
13. Z.-K. Tan, R. S. Moghaddam, M. L. Lai, P. Docampo, R. Higler, F. Deschler, M. Price, A. Sadhanala, L. M. Pazos, D. Credgington, F. Hanusch, T. Bein, H. J. Snaith, and R. H. Friend, "Bright light-emitting diodes based on organometal halide perovskite," Nat. Nanotechnol. **9**(9), 687–692 (2014).
14. W. Zhang, M. Saliba, S. D. Stranks, Y. Sun, X. Shi, U. Wiesner, H. J. Snaith, and H. J. Snaith, "Enhancement of perovskite-based solar cells employing core-shell metal nanoparticles," Nano Lett. **13**(9), 4505–4510 (2013).
15. L. Yue, B. Yan, M. Attridge, and Z. Wang, "Light absorption in perovskite solar cell: Fundamentals and plasmonic enhancement of infrared band absorption," Sol. Energy **124**, 143–152 (2016).

#265320 http://dx.doi.org/10.1364/OE.24.020696
Journal © 2016 Received 17 May 2016; revised 24 Jul 2016; accepted 26 Jul 2016; published 30 Aug 2016

Optics EXPRESS

16. M. Saliba, W. Zhang, V. M. Burlakov, S. D. Stranks, Y. Sun, J. M. Ball, M. B. Johnston, A. Goriely, U. Wiesner, and H. J. Snaith, "Plasmonic-induced photon recycling in metal halide perovskite solar cells," Adv. Funct. Mater. **25**(31), 5038–5046 (2015).
17. R. Wu, B. Yang, C. Zhang, Y. Huang, Y. Cui, P. Liu, C. Zhou, Y. Hao, Y. Gao, and J. Yang, "Prominent efficienty enhancement in perovskite solar cells employing silica-coated gold nanorods," J. Phys. Chem. C **120**(13), 6996–7004 (2016).
18. S. Carretero-Palacios, M. E. Calvo, and H. Míguez, "Absorption enhancement in organic-inorganic halide perovskite films with embedded plasmonic nanoparticles," J Phys Chem C Nanomater Interfaces **119**(32), 18635–18640 (2015).
19. E. S. Arinze, B. Qiu, G. Nyirjesy, and S. M. Thou, "Plasmonic nanoparticle enhancement of solution-processed solar cells: Practical limits and opportunities," ACS Photonics **3**(2), 158–173 (2016).
20. Z. Sun, L. Aigouy, and Z. Chen, "Plasmonic-enhanced perovskite-graphene hybrid photodetectors," Nanoscale **8**(14), 7377–7383 (2016).
21. D. Gurudayal, D. Sabba, M. H. Kumar, L. H. Wong, J. Barber, M. Grätzel, and N. Mathews, "Perovskite-hematite tandem cells for efficient overall solar driven water splitting," Nano Lett. **15**(6), 3833–3839 (2015).
22. Y. J. Li, Y. Lv, C.-L. Zou, W. Zhang, J. Yao, and Y. S. Zhao, "Output coupling of perovskite lasers from embedded nanoscale plasmonic waveguides," J. Am. Chem. Soc. **138**(7), 2122–2125 (2016).

1. Introduction

In the past several years, solar cells based on solution-processed organic-inorganic metal-halide perovskites have been received extensive research interests due to the excellent material properties in high aborption efficiency and cost-effective fabrication processes to dominate the next generation of photovoltaics market. Since Kojima *et al*. first proposed to replace the dye with a layer composed of the perovskites in dye-sensitized solar cells in 2009, the photo-conversion efficiency of the proposed perovskite-based solar cells has been promoted to a remarkable milestone of more than 20% [1–6]. Moreover, advanced studies have shown that the photoluminescence (PL) quantum efficiencies in perovskites exceed 70% and the lasing wavelengths may be altered with different halide conponents in perovskite compositions [7,8]. These advanced light emitting properties make the perovskites as alternative materials not only for the photovoltaics applications, but also the great capabilities in light-emitting devices such as the efficient on-chip coherent light sources and white-light light-emitting diodes [9–13].

As of today, several effective routes have been developed to incorporate metallic nanoparticles into perovskite-based solar cells, with most reports attributing the significant photo-conversion efficiency improvement to the increased light absorption through plasmonic effects. For example, the near-field electric field enhancement resulted from the surface plasmon excition of the constitute metallic nanostructures such as $Au@SiO_2$ core-shell nanoparticles and nanorods can be employed to promote the effective light absorption cross-section of solar cells. Also, the light scattering from the plasmonic metal nanoparticles may be a medium for the redirection of light into solar cell devices by increasing the optical path-length. Moreover, the metallic nanoparticles can be directly utilized as sensitizers to harvest light and inject photoninduced electrons to an electron acceptor [14–19]. The surface plasmonic effect of utilizing metallic nanostructures is a promising method to boost the optoelectronic device performance.

In addition to the expolitations in photovoltaics components, several advanced applications of using perovskite materials incorporated with the plasmonic effects have been proposed and demonstrated such as the high-responsivity perovskite-graphene photodetector via the insertion of gold nanoparticles to doubly enhance the photoresponse speed and the overall unassistated water splitting device with perovskite-hematite tandem cells to achieve a solar-to-hydrogen conversion efficiency of 2.4% [20,21]. Regarding the lasing devices, Li *et al.* proposed a perovskite laser integrated with Ag nanowire plasmonic waveguides, forming rationally designed prevoskite/silver heterostructures. Via the photon-plasmon coupling, such an integrated devices can be employed to successfully extract the lasing modes in form of surface plasmon. Meanwhile, the output lasing modes can be efficiently modulated by controlling the resonant modes of the perovsite microcavities [22].

The electron-photon interaction processes in the hybrid organic-inorganic perovskite materials are intrinsically complex. They may be influenced by not only the material

Optics EXPRESS

properties which may be acquired from different fabrication processes, but also the device component configurations for different optoelectronic applications, causing intricate interactions in structural disorders and surrounding materials. Furthermore, regarding the practical applications, the serious perovskite material quality degradation from the hydrolysis in ambient environment may be one of the most critical problems and urgent to be solved. In this paper, we exploit a transparent thermoplastic layer of polymethylmethacrylate (PMMA) capped onto the as-prepared perovskite layer to prevent the sample damages from the hydrolysis. Furthermore, with a continuous Ag thin film evaporated on the samples, the coherent light emission properties can be promoted with greatly reduced lasing threshold excition powers due to a better confinement of plasmonic fields.

2. Perovskite fabrications

The solution-processed organic-inorganic metal-halide perovskite thin films were prepared in a two-step sequential deposition process. First, the powdered lead iodide (PbI_2, Sigma-Aldrich) was completely dissolved in *N*, *N*-dimethylformamide (DMF) and kept stirring at 60 °C inside a nitrogen-filled glove box in order to avoid the PbI_2 precipitation. Then in the perovskite film fabrication process, the as-prepared PbI_2 solution was deposited onto a 70 °C UV-O_3-cleaned glass substrate by spin-coating 6000 rpm for 30 seconds. The coated solution was subsequently dried at 80 °C for 15 minutes, forming a yellow PbI_2 film on the substrate surface. Next, a 1 wt% precursor solution of methylammonium iodide (MAI, CH_3NH_3I) in 2-propanol (IPA) was spin-coated onto the PbI_2 film at room temperature and then gradually dried in 40 seconds to remove the solvent completely. The resulting films were annealed at 100°C for 2 hours for the complete interdiffusion of the the two precursor components, generating large-scale dark-brown $CH_3NH_3PbI_3$ perovskite layers. The top-view scanning electron microscope (SEM) image of the fabricated perovskite film is shown in Fig. 1(a). As presented in the image, air-vacancies are formed in the perovskite sample, forming inhomogeneous rugged surface and randomly distributed grain boundaries. The thickness of the perovskite film is in a range of 100-300 nm with an average of 250 nm. The film morphology and the ratio of the air-vacancy occupation to the total area can be manipulated by controlling the PbI_2 solution concentration and the adding process of the MAI solution.

To further look into the structural configurations of the perovskite films, the transmission electron microscope (TEM) analyses were conducted and the corresponding image is shown in Fig. 1(b). The perovskite films consist nanocrystalline structures which are densely distributed as inclusions in perovskites and orient in the (110) crystal direction. The main nanocrystal size distribution is in a range of 6-10 nm. After the perovskite film preparation, a transparent thermoplastic layer of polymethylmethacrylate (PMMA) and a continuous silver (Ag) thin film were directly spin-coated and e-beam evaporated onto the prepared perovskite films, respectively. The layer structure is schematically demonstrated in Fig. 1(c). The PMMA film is at around 20 nm in thickness and can be used as a protective layer to prevent the perovskite degradation from the hydrolysis in ambient environment, acquiring stable material quality and long-lasting light-emitting performance. The thickness of the Ag thin film is about 50 nm. Since both the PMMA and Ag films are relatively thin compared to the roughness of the fabricated perovskite films, the surface profile of the Ag thin layer may be changed with the thickness variation of the perovskite films, resulting in localized plamonics fields generated between the Ag and perovskite films.

Optics EXPRESS

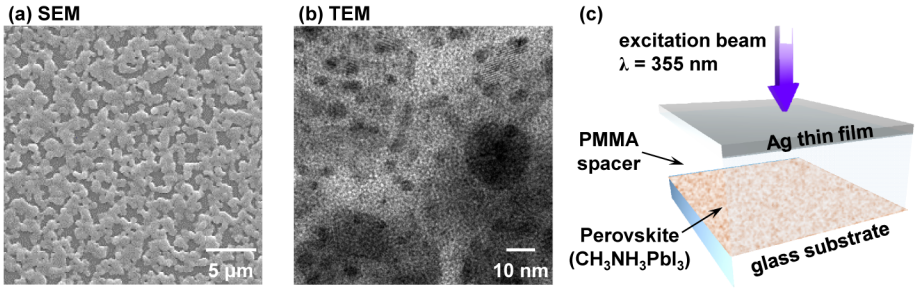

Fig. 1. Structural configurations of the solution-processed $CH_3NH_3PbI_3$ perovskites. (a) Top-view SEM image of the as-prepared perovskite film morphology. (b) The corresponding TEM image shows that the nanocrystalline structures exist and form randomly distributed grain boundaries in perovskite films. (c) Schematic layer structure of the solution-processed perovksites capped with a dielectric PMMA spacer and a Ag thin film.

3. Optical characterizations

To investigate the lasing performance of the hybrid perovskite configuration with capped PMMA and Ag thin films, the power-dependent photoluminescence (PL) measurements were conducted using a third harmonic generation (THG) of a Nd:YVO_4 pulse laser as an optical excitation source. The excitation wavelength is 355 nm, while the pulse duration and the repetition rate are 0.5 ns and 1 kHz, respectively. By launching the laser light beam into a microscope objective lens of 0.55 N.A., the focal spot size can be concentrated at around 15 μm in diameter and focused on the perovskite sample surface. Figure 2(a) shows the coherent light emission properties of the hybrid perovskite sample in a range of the excitation power changed from 2 μW to 40 μW at a low environment temperature of 77 K. With a gradual increase of the excition powers, the peak intensity dramatically increases as the incident pumping power exceeds around 10 μW. The central wavelength of the emission peak occurs at about 753 nm. Such an emission wavelength can be referred to the orthorhombic phase state of the perovskite films at a low ambient temperature.

The corresponding linewidth at full width at half maximum (FWHM) of the emission peaks from the hybrid perovskite configuration is down to around 3 nm from ~10 nm as the pink line indicated in Fig. 2(b). Therefore, both the nonlinear peak intensity varation in light-light curve and the significant reduction in the peak width show the lasing behavior of the perovskite films covered with a Ag thin film and a PMMA dielectric layer. The lasing threshold power can be estimated at around 10 μW. Compared to the layer configurations of the perovskite thin films directly capped with a Ag thin film (green) and the bare perovskites on glass substrates (blue), the hybrid perovskite configuration exchibits a better lasing performance. The threshold pumping power is less than one or two orders of the magnitudes in the other two types of sample configurations. The lasing action of the perovskite films results from the multiple random scattering between the grain boundaries in perovskites [11]. The adding PMMA and Ag thin films may provide the strong field confinement, resulting in a significant improvement on the reduction of the lasing threshold excitation power. Therefore rough perovskite morphology may provide larger surface area to volume ratio, causing more perovskite-PMMA-Ag hybrid structure configurations in the exciton-plasmon scheme. Factors to be considered in the optimization of the perovskite lasing performance shall include not only the perovskite morphology roughness, but also the amount of perovskite, perovskite nanocrystal size, the thickness of the adding dielectric and metallic layers, etc. We also found that light-emitting performance of the perovskite sample with the hybrid structure configuration maintains for a longer period of time. The light-emitting intensity would drop around 20% after 10 days. This durability cannot be observed in the bare perovskite samples, which may degrade from the hydrolysis reaction in one day. Moreover, the sandwiched dielectric PMMA layer may provide as a spacer to modulate the exciton-plasmon coupling strength between the Ag and perovskite films. The PMMA layer also can be used to prevent

Optics EXPRESS

the direct quench of the perovskite nanocrystallne structures from the localized plasmonic fileds in the vicinity of the Ag thin film. A series of calculations on the plasmonic mode analyses and the experiments on the lasing perforamance of the hybrid perovskite configuration with different PMMA thicknesses will be conducted and discussed in the following sections.

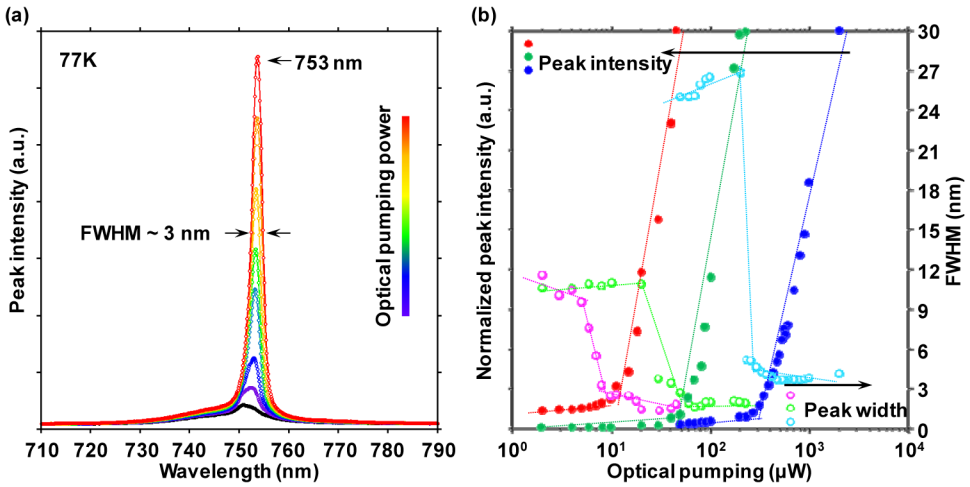

Fig. 2. Optical characterizations of different sample configurations with perovskite thin films. (a) PL emission spectra of the hybrid perovskite configuration with capped PMMA and Ag thin films. The excitation power is a range from 2 μW to 40 μW. The central wavelength of the coherent light emission is at about 753 nm. (b) Comparison of the lasing actions of different layer configurations with the provskite thin films. The L-L curves plotted in a log-linear scale and the corresponding linewidths as a function of the excitation powers. (Red: perovskite films with capped PMMA and Ag thn films; Green: perovskite films cover with a Ag thin film; Blue: bare perovskite films on glass substrates)

4. Plasmonic mode analyses

To analyse the plasmonic mode in the hybrid perovskite configuration capped with Ag and PMMA thin films, theoretical simulations of the field distributions in the perovskite layer and the vicinity of the Ag thin film were conducted by using the finite element method (FEM, COMSOL Multiphysics). In the simulation models, we considered the three layer configurations as shown in Fig. 3; that is (a) bare perovskite films on glass substrate, (b) perovskite layer directly covered with a Ag thin film; and (c) PMMA dielectric layer of 20 nm sandwiched between the Ag and perovskite layers. The realistic material parameters and Joule loss factors of the constituent materials are obtained from a well-established database of the dielectric parameters. The thicknesses of different material layers are extracted from the real sample geometry, while the layer thickness variation is estimated to be ± 40 nm. In the simulations, we performed the simulation model of the perovskite film morphology in a rough and continuous condition, while the surface profile variation was extracted from the real perovskite sample geometry in a small segment. The PMMA and the Ag thin films are changed along with film morphology variation of the underneath perovskites. Therefore, this simulation model may be quite close to the real samples while the PMMA thickness is 20 nm. The wavelength of an incident excitation light beam is corresponding to the light emission properties of the perovskite sample configurations. As the calculated field intensity distributions shown in Fig. 3(c), enhanced optical field confinement occurs in the hybrid perovskite configuration, giving an enhancement factor of 19.3 and 7.7 as compared to the layer configurations in Fig. 3(a) and 3(b), respectively.

The significant field enhancement may result from the induced localized surface plasmon. In the localized surface plasmon resonance state, the free electrons oscillate with the

Optics EXPRESS

maximum amplitude, exhibiting intense and spatially non-homogeneous oscillating electrical fields in the vicinity of the plasmonic nanostructures or the structures with sharp features. Therefore, the energy of the incident light irradiation is transferred and localized in the near-field region of the nanostructures. It is also found that the induced plamonic fields can enhance the charge carrier generation of adjacent semiconductor nanocrystals with an overlapping of the localized surface plasmon and the bandgap energies. Under such a circumstance, a strong electric field is expected to generate between the plasmonic nanostructures and the constitute semiconductor nanocrystal with proper spacing distance, whose intensity can be enhanced up to several orders of magnitude larger than that of the far-field incident light. Thus, with an introduction of plasmonic conponents, the requied excitation power for lasing action in perovskite film may be greatly reduced due to the local enhanced electric field.

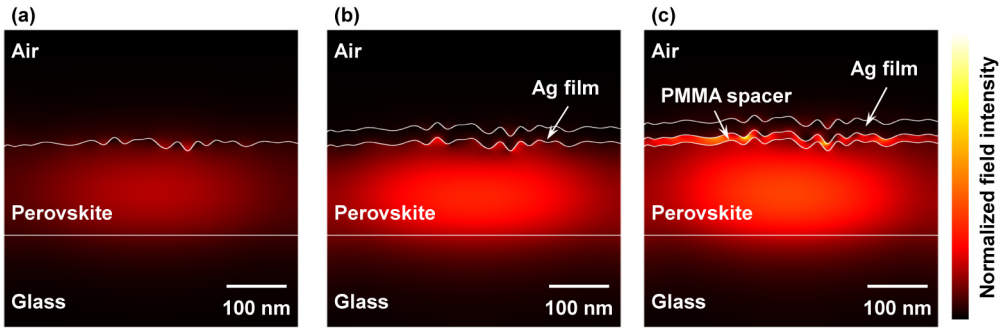

Fig. 3. Comparisons of the field intensity distributions at different layer configurations. (a) bare perovskite films on glass substrate, (b) perovskite layer directly covered with a Ag thin film; (c) PMMA dielectric layer of 20 nm sandwiched between the Ag and perovskite layers.

5. Comparison of lasing performance within different configurations

Figure 4(a) shows the comparison of the threshold excitation power for lasing actions at different layer configurations with perovskites. Also, the hybrid perovskite configurations with PMMA layer at different thicknesses are taken into account. As described in the above simulation results, the best lasing performance of the perovskite films is the perovkiste film covered with the PMMA dielectric layer and the Ag thin film. The threshold excitation power of the lasing action in perovskite films is much less than that in the configurations of bare perovskite films on glass substrates and the perovskite directly coated with Ag thin film. Due to the simulation results, the enhanced optical confinement may result from the induced localized plasmonic field in the vicinity of the Ag thin film. Therefore, with an increase of the thickness of the PMMA dielectric spacer, the enhanced field confinement may result from the multiple reflection between the interface of the Ag and perovskite thin films. According to the acquired results, we found that the lasing peak position and the peak width may be irrelevant to the thickness variation of the PMMA layer. Only the threshold excitation powers are changed with the PMMA thickness variation as described above. Thus, with the capped PMMA and Ag thin films, the lasing performance may be improved with a significant reduction of the lasing threshold power.

Moreover, the coherent light emission properties can be enhanced and performed at room temperature within the hybrid perovskite configuration as the results demonstrated in Fig. 4(b) in a range of the excition power of 225 μW to 4 mW. With a gradual increase of the excition powers, the peak intensity dramatically increases as the incident pumping power exceeds around 400 μW. Although the threshold excitation power is high, such an enhance coherent light emission properties were not observed in previous studies. The PL emission spectra exhibit an emission peak occurred at around 787 nm, corresponding to the tetragonal phase state of the perovskite film at room-temperature.

Optics EXPRESS

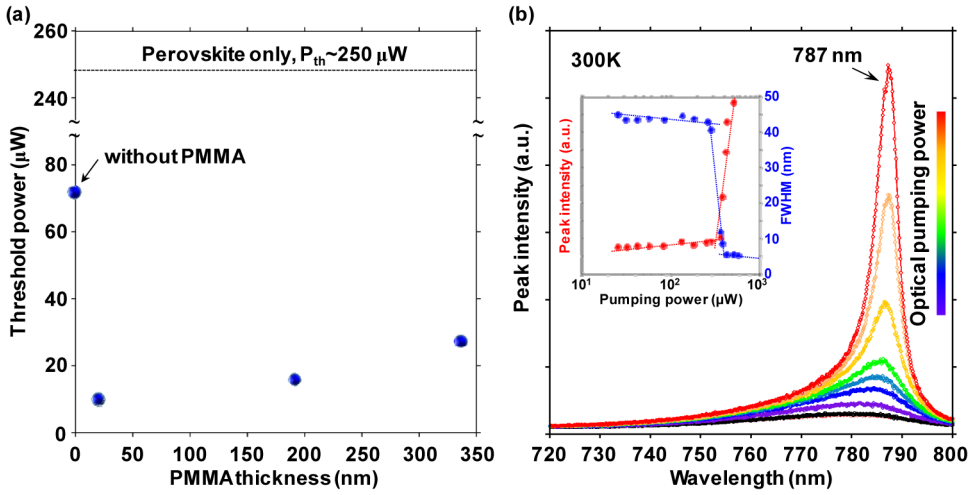

Fig. 4. Comparison of lasing performance with different configurations. (a) Excitation powers for lasing action with different layer configurations and the hybrid perovskite configuration with PMMA layer at different thickness. (b) Coherent light emission properties of the hybrid perovskite configuration at room temperature (300K). The excitation power is a range from 225 μW to 4 mW. The central wavelength of the coherent light emission is at about 787 nm.

6. Conclusions

In conclusion, with the adding Ag and PMMA thin films on prepared solution-processed organic-inorganic lead-halide perovskite $CH_3NH_3PbI_3$ films, the low-tempearture lasing performance can be greatly promoted with the threshold excition power reduced by over two orders of magnitude than that obtained in bare peroskite layers. Via the theoretical simulations, strong exciton-plasmon coupling occurs between the Ag and perovskite thin films, ascribing to the induced plasmonic fields localized in the vicinity of the Ag thin film. The confined optical fields between the Ag and perovskite films can be enhanced by about 19.3 and 7.7 times as compared to the layer configurations of bare perovskites on glass substrates and perovskites with coating Ag thin film, respectively. The sandwiched dielectric PMMA layer may provide as a spacer to modulate the exciton-plasmon coupling strength between the Ag and perovskite films. The PMMA layer also can be used to prevent the direct quench of the perovskite nanocrystallne structures from the localized plasmonic fileds in the vicinity of the Ag thin film and exploited to prevent the perovskite degradation from the hydrolysis in ambient environment, achieving stable material quality and long-lasting light-emitting performance. Moreover, the room-temperature coherent light emission properties can be enhanced and performed by exploiting the hybrid perovskite configuration with the adding Ag and PMMA films, paving new perspectives towards the promising applications of laser devices with solution-processed perovskites.

Funding

This work was partially supported by the Ministry of Education Aim for the Top University program and by the Ministry of Science and Technology of Taiwan under Contract Nos. MOST 104-2221-E-009-096-MY3, MOST 104-2221-E-009-094-MY3 and MOST 104-2218-E-009-026.

Acknowledgments

We acknowledge the help of Prof. S. C. Wang and Prof. H. C. Kuo at National Chiao Tung University for contributing fruitful discussions and technical support.